HIV-1 Protease Inhibitors Nelfinavir and Atazanavir Induce Malignant Glioma Death by Triggering Endoplasmic Reticulum Stress

Peter Pyrko,[1] Adel Kardosh,[2] Weijun Wang,[4] Wenyong Xiong,[3] Axel H. Schönthal,[2] and Thomas C. Chen[4]

Departments of [1]Pathology, [2]Molecular Microbiology and Immunology, [3]Physiology and Biophysics, and [4]Neurosurgery, University of Southern California Keck School of Medicine, Los Angeles, California

Abstract

HIV type 1 (HIV-1) protease inhibitors (PI) have been shown to have anticancer activity in non–HIV-associated human cancer cells. The underlying mechanism of this effect is unclear. Here, we show that the PIs nelfinavir and atazanavir cause cell death in various malignant glioma cell lines *in vitro*. The underlying mechanism of this antitumor effect involves the potent stimulation of the endoplasmic reticulum (ER) stress response (ESR), as indicated by increased expression of two ESR markers, GRP78 and CHOP, and activation of ESR-associated caspase-4. Induction of ESR seems to play a central role in PI-induced cell death because small interfering RNA–mediated knockdown of the protective ER chaperone GRP78 sensitizes cells; whereas knockdown of proapoptotic caspase-4 protects cells from PI-induced cell death. Furthermore, the treatment of cells with PIs leads to aggresome formation and accumulation of polyubiquitinated proteins, implying proteasome inhibition. Thus, our results support a model whereby PIs cause tumor cell death via triggering of the ESR, inhibition of proteasome activity, and subsequent accumulation of misfolded proteins. Inhibition of glioma growth via ESR takes place in the *in vivo* setting as well, as nelfinavir inhibits the growth of xenografted human malignant glioma, with concomitant induction of the proapoptotic ER stress marker CHOP. Because ER stress has also been reported as the mechanism for insulin resistance and diabetes, our ER stress model of PI function may also explain why these drugs may induce insulin resistance as one of their most common side effects. [Cancer Res 2007;67(22):10920–8]

Introduction

HIV type 1 (HIV-1) protease inhibitors (PI) have become important tools in the treatment of HIV infection and include nelfinavir (Viracept), sequinavir (Invirase), ritonavir (Norvir), amprenavir (Agenerase), indinavir (Crixivan), and atazanavir (Reyataz). The addition of these drugs to highly active antiretroviral therapy (HAART) has improved patient outcomes and decreased viral resistance (1). Moreover, the treatment with ritonavir, indinavir, or sequinavir has had an unexpected additional consequence, the regression of Kaposi's sarcoma (2), which prompted researchers to investigate the potential antitumor effects of protease inhibitors in various other cancer models. Since then, several reports indicated that PIs might indeed harbor antitumor activity, albeit to varying degrees. For example, indinavir has been shown to reduce the invasion of hepatocarcinoma cell lines *in vitro* and to delay growth of these tumors in a nude mouse model *in vivo* (3). Using prostate carcinoma cell lines, Yang et al. (4) reported that nelfinavir was able to block interleukin-6–stimulated signal transduction pathways *in vitro* and inhibited xenograft tumor growth *in vivo*. In an investigation with ritonavir, sequinavir, and nelfinavir, all three drugs were shown to induce growth arrest and apoptosis in multiple myeloma cells *in vitro* (5). Furthermore, ritonavir was shown to inhibit EL4-T cell thymoma growth in syngeneic mice (6). However, in a study using an established glioblastoma cell line, Laurent et al. (7) observed that ritonavir failed to inhibit tumor growth *in vivo*, although the drug did display cytostatic and cytotoxic effects *in vitro*.

An additional feature of protease inhibitors that might be beneficial for their potential use as anticancer agents is their ability to sensitize cancer cells to radio- and chemotherapy. For example, saquinavir, ritonavir, and indinavir were shown to potentiate the effects of all–*trans*-retinoic acid on human myelocytic leukemia cells (8), and ritonavir was shown to enhance the anticancer effects of docetaxel on prostate cancer cells *in vitro* and *in vivo* (9). Other investigators showed that the treatment of prostate, glioblastoma, and leukemia cells with saquinavir caused the induction of apoptosis, and that sequinavir sensitized prostate cancer cells to ionizing radiation (10). Nelfinavir and amprenavir were also shown to decrease vascular endothelial growth factor (VEGF)/HIF-1α expression and angiogenesis in glioblastoma cells (11), whereas nelfinavir induced cell cycle arrest and apoptosis in melanoma cells (12). In addition, amprenavir and nelfinavir increased the effectiveness of radiotherapy in an animal xenograft tumor model (13). Although various mechanisms have been proposed to explain the antitumor effects of the different protease inhibitors, such as inhibition of nuclear factor κB (NF-κB; ref. 14), blockage of Akt signaling (4, 13), or inhibition of cytochrome P450 3A4 enzyme (CYP 3A4; ref. 9), this issue has not been convincingly clarified.

In this present study, we present evidence that protease inhibitors might impair tumor cell growth via the stimulation of a particular stress pathway, called the endoplasmic reticulum (ER) stress response (ESR) or unfolded protein response (UPR). The ESR consists of a set of adaptive pathways that can be triggered by disparate perturbations in normal ER function, such as accumulation of misfolded proteins, lipid or glycolipid imbalances, or changes in the ionic conditions of the ER lumen (see refs. 15, 16 for reviews). The primary purpose of the ESR is to alleviate the stressful disturbance and restore proper ER homeostasis. In the case of intense or persistent ER stress, however, these pathways will trigger programmed cell death/apoptosis. One of the central prosurvival regulators of the ESR is glucose-regulated protein 78 (GRP78/BiP), which has important roles in protein folding and

Requests for reprints: Thomas C. Chen, Department of Neurosurgery, University of Southern California Keck School of Medicine, 1200 N State St. #5046, Los Angeles, CA 90033. Phone: 323-226-7421; Fax: 323-226-7833; E-mail: tcchen@usc.edu.

doi:10.1158/0008-5472.CAN-07-0796

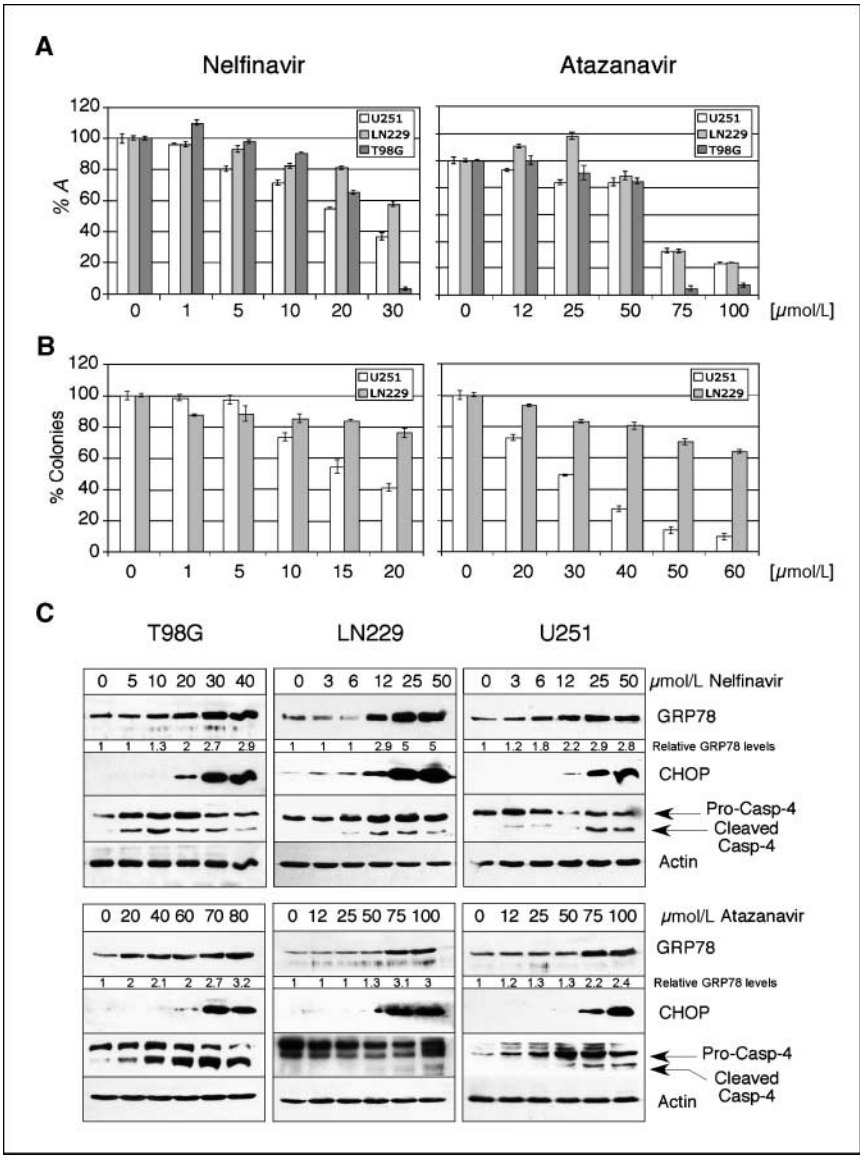

Figure 1. Protease inhibitors inhibit glioblastoma cell growth as well as survival and induce ER stress markers *in vitro. A,* U251, T98G, and LN229 glioblastoma cell lines were exposed to increasing concentrations of nelfinavir and atazanavir. Cells cultured in 96-well plates were treated with drugs for 48 h, and cell growth and survival were determined by conventional MTT assay. MTT assays were done in 96-well plates with the use of 3.0 to 8.0 $\times$ 10^3 cells per well as described in detail elsewhere (50). Cell viability of untreated cells was set at 100%. *Columns,* mean; *bars,* SE; n = 8. Because the MTT assay is based on the measurement of the metabolic activity of the cell culture, drug effects were also determined via cell counts over time, as well as by visual inspection of drug-treated cultures (data not shown); these additional approaches excluded general metabolic interference as a major cause for the outcome shown in this figure, but rather, confirmed that these drugs effected overall reduced cell growth and survival. *B,* 300 cells per well were seeded in six-well plates and treated with the indicated drug for 48 h. Thereafter, the medium was replaced with fresh medium, and the cells were allowed to proliferate for 14 d in the absence of the drug. The newly formed colonies of adherent cells were stained with methylene blue and counted. The number of colonies formed in the absence of drug treatment was set at 100%. *Columns,* mean; *bars,* SE; n = 6. Because T98G cells are not able to spawn colonies under these conditions, they were not included in this part of the experiment. *C,* U251, T98G, and LN229 glioblastoma cell lines were cultured in the presence of increasing concentrations of nelfinavir and atazanavir for 48 h. Cellular lysates were prepared and subjected to Western blot analysis with antibodies to ER stress markers GRP78, CHOP, and caspase-4. The levels of GRP78 protein were quantified using ImageJ software. Actin antibody was used as a loading control to verify equal amounts of lysate in each lane.

assembly, in targeting misfolded proteins for degradation, in ER Ca^{2+} binding, and in controlling the activation of transmembrane ER stress sensors (17). On the other hand, CCAAT/enhancer binding protein homologous transcription factor (CHOP/GADD153) and caspase-4 are critical executioners of the proapoptotic arm of the ESR (18, 19).

In this study, we show that nelfinavir and atazanavir are able to potently induce ESR in malignant glioma cells, as indicated by elevated levels of GRP78 and CHOP, and activation of caspase-4, which leads to cell death. Moreover, both drugs cause the accumulation of polyubiquitinated proteins and subsequent aggresome formation, consistent with our view that ER stress is due to proteasome inhibition, with resultant accumulation of misfolded proteins. This notion is further supported by our observation that inhibition of general protein synthesis (which prevents an increase in misfolded proteins) abrogates the ESR-stimulatory effects of both nelfinavir and atazanavir. Taken together, our study suggests that protease inhibitors might exert their anticancer activity via the stimulation of ER stress with resultant cell death.

Materials and Methods

Materials. Nelfinavir (Viracept, 625 mg) was purchased from Agouron Pharmaceuticals Inc., whereas atazanavir (Reyataz, 150 mg) was purchased from Bristol-Myers Squibb Company. The pills were ground and dissolved in 100% ethanol at 25 mmol/L (stock solution). Both drugs were added to the cell culture medium in a manner that kept the final concentration of solvent (ethanol) below 0.8%. Appropriate amount of ethanol (based on the highest concentration of solvent added with the drugs) was always added to the controls.

Cell lines and culture conditions. The malignant glioma cell lines U251 and LN229 were provided by Frank B. Furnari and Webster K. Cavenee (Ludwig Institute of Cancer Research, La Jolla, CA). T98G and U87 malignant glioma cell lines were obtained from the American Tissue Culture Collection. All cell lines were propagated in DMEM (Life Technologies BRL) supplemented with 10% fetal bovine serum, 100 units/mL penicillin, and 0.1 mg/mL streptomycin in a humidified incubator at 37°C and a 5% CO_2 atmosphere.

Immunoblots and antibodies. The cells were lysed in radioimmunoprecipitation assay buffer (RIPA), and equal amounts of total cellular lysates were processed by Western blot analysis according to established procedures (20). Antibodies to GRP78 and CHOP and caspase-4 were

obtained from Santa Cruz Biotechnology, Inc. and were used according to manufacturer's recommendations. Caspase-4 was also purchased from StressGen Biotechnology Corporation. The secondary antibodies were coupled to horseradish peroxidase and were detected by chemiluminescence using the SuperSignal West substrate from Pierce. All immunoblots were repeated at least once to confirm the results. The GRP78 blots were quantified using ImageJ software (21).

Immunohistochemistry. Immunohistochemical analysis of protein expression in tumor tissues was done with the use of the Vectastatin ABC kit (Vector Laboratories) according to manufacturer's instructions.

Terminal nucleotidyl transferase–mediated nick end labeling assay. Apoptosis in tumor sections was assessed with the use of the terminal nucleotidyl transferase–mediated nick end labeling (TUNEL) assay (22). All components for this procedure were from the ApopTag *In situ* Apoptosis Detection kit (Chemicon), which was used according to the manufacturer's instructions. Hematoxylin was used for background staining.

Colony formation assay. Twenty-four hours after transfection with small interfering RNA (siRNA), the cells were seeded into six-well plates at 200 cells per well. After complete cell adherence, the cells were exposed to drug treatment for 48 h. Thereafter, the drug was removed, fresh growth medium was added, and the cells were kept in culture undisturbed for 12 to 14 days, during which time the surviving cells spawned a colony of proliferating cells. Colonies were visualized by staining for 4 h with 1% methylene blue (in methanol) and then were counted.

Electron microscopy. Electron microscopy was done by the Doheny Eye Institute Specialized Microscopy Core Facility at the University of Southern California. Cells were spun down into a beam capsule with a clinical centrifuge. Pelleted cells were fixed in 2% paraformaldehyde and 0.1% glutaraldehyde in 0.1 mol/L phosphate buffer (pH, 7.4) at room temperature for 1 h. The cell pellets were then postfixed with 1% osmium tetroxide for 2 h on ice and then rinsed thrice with distilled water. The fixed pellets were dehydrated through an ethanol dilution series up to 100% ethanol and then immersed in propylene oxide (PO) thrice for 2 min. Pellets were then infiltrated in a 3:1 PO/Eponate resin mixture overnight. The pellets were then embedded in 100% Eponate resin (Ted Pell Inc.) in beam capsules and placed in a 60°C oven overnight. After hardening, tissue blocks were ultrathin sectioned at 75 nm thickness and placed on 300 mesh copper grids. Grids were next counterstained with saturated uranyl acetate and lead citrate and then analyzed on a Zeiss EM 10 electron microscope (Zeiss).

Transfections with siRNA. Cells were transfected in six-well plates with the use of LipofectAMINE 2000 (Invitrogen) according to manufacturer's instructions. The different siRNAs were synthesized at the microchemical core laboratory of the USC/K. Norris Jr. Comprehensive Cancer Center, and their sequences were as follows; si-GFP (sense): 5′-CAAGCUGACCCUGAAGUUCTT-3′; (antisense): 5′-GAACUUCAGGGUCAGCUUGTT-3′; si-GRP78 (sense): 5′-GGAGCGCAUUGAUACUAGATT-3′; (antisense): 5′-UCUAGUAUCAAUGCGCUCCTT-3′; si-Caspase-4 (sense): 5′-AAGUGGCCUCUUCACAGUCAUTT-3′; (antisense): 5′-AAAUGACUGUGAAGAGGCCACTT-3′.

Cytoplasmic calcium imaging. The cells were loaded by incubating them with 4 μmol/L Fura-2/AM (Invitrogen) for 30 min at room temperature in external solution containing 138 mmol/L NaCl, 5.6 mmol/L KCl, 1.2 mmol/L $MgCl_2$, 2.6 mmol/L $CaCl_2$, 10 mmol/L HEPES, and 4 mmol/L glucose (pH, 7.4). After loading, the cells were rinsed and transferred to the imaging setup. The cells were treated with individual drugs for 10 s, whereas fluorescence was elicited with the excitation wavelength alternating between 350 and 380 nm, using a Polychromator V (TILL Photonics GmbH) to provide illumination via a Zeiss Axiovert 100 microscope with a Zeiss Fluar 40× oil objective (Carl Zeiss). Images were captured using a Cascade 512B CCD camera (Photometrics) controlled with MetaFluor software (Molecular Devices) at 0.5 Hz acquisition frequency. Ratios of the images obtained at 350 nm and 380 nm excitation were used to illustrate changes in the cytoplasmic calcium concentration according to the principles developed by Tsien (23).

Tumor growth in nude mice. Male athymic *nu/nu* mice 4 to 6 weeks old were obtained from Harlan and implanted s.c. with 5×10^5 U87 glioblastoma cells as described in detail elsewhere (24). For the determination of tumor growth during continuous drug treatment, 40 mg/kg nelfinavir was given via direct administration into the stomach

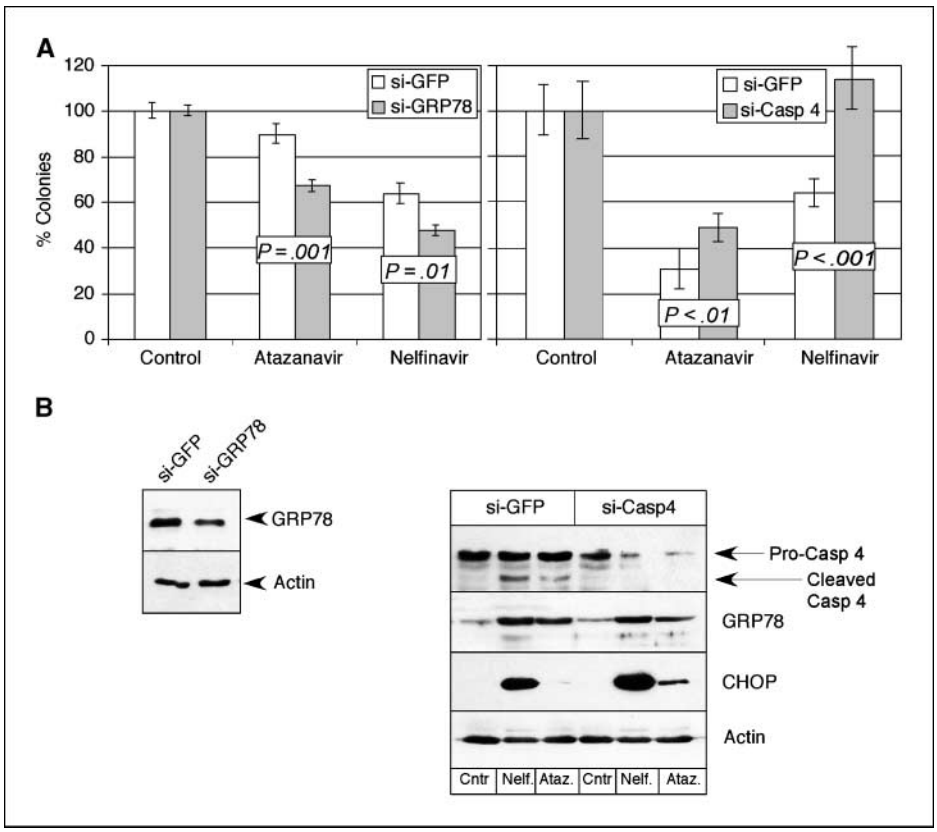

Figure 2. Knockdown of GRP78 enhances, whereas knockdown of caspase-4 reduces, cell killing by nelfinavir and atazanavir. U251 glioblastoma cells were transiently transfected with siRNA directed at GRP78 (si-GRP78) or caspase-4 (si-Casp 4). As a control, siRNA targeted at green fluorescent protein (si-GFP) was used. *A,* 48 h after transfection, parallel cultures were treated with 15 μmol/L nelfinavir and 25 μmol/L atazanavir in the case of si-GRP78/si-GFP or with 30 μmol/L nelfinavir and 50 μmol/L atazanavir in the case of si-Casp 4/si-GFP. In all instances, control cultures received no drug treatment or treatment with solvent (ethanol) alone. After 48 h of drug treatment in the case of siGRP78 and 36 h in the case of siCasp4, the drugs were removed, and the fraction of surviving cells was determined by colony-forming assays. Shown is the percentage of surviving cells (where the number of colonies under non–drug-treated conditions was set to 100%). The *P* values show statistically significant differences in survival between cells receiving si-GRP78 and control siRNA (*si-GFP*) and between cells receiving si-Casp 4 and control siRNA, respectively. *B,* to verify the effectiveness of the siRNAs, Western blot analysis of the respective target proteins was done. Additionally, in the case of the caspase-4 knockdown, the effects on GRP78 and CHOP protein levels were determined. This experiment was done in parallel to colony-forming assays, and the same concentrations of drugs were used.

with a stainless-steel ball-head feeding needle (Popper and Sons Inc.) in 25% ethanol, and tumor growth was monitored and recorded as described (24). For the examination of short-term *in vivo* effects of drugs on CHOP expression, the animals received a daily dose (120 mg/kg) of the drug in the same way. Ninety-six hours later, the animals were sacrificed, and the tumors were harvested for analysis.

Results

To establish the effects of nelfinavir and atazanavir on malignant glioma cells *in vitro*, we did conventional 3-(4,5-dimethylthiazol-2-yl)-2,5-diphenyltetrazolium bromide (MTT) assays, which measured short-term growth and survival of the treated cell culture, as well as colony-forming assays, which revealed the ability of individual cells to survive and develop a new colony. We picked three glioblastoma cell lines (U251, LN229, T98G) based on their different genetic background. First, the cell lines were cultured in 96-well plates in the presence of nelfinavir and atazanavir for 48 h, and cell proliferation was determined using MTT assay. Both drugs inhibited cell growth in all cell lines in a concentration-dependent manner (Fig. 1*A*). Although the sensitivity to these drugs differed from cell line to cell line, the overall viability was significantly decreased in all cell lines used. In addition, the inhibitory effects of nelfinavir seemed to be more potent than those of atazanavir. Second, colony-forming assays were done with U251 and LN229 cells. As shown in Fig. 1*B*, both drugs decreased cell survival, and nelfinavir again was more effective than atazanavir.

Interestingly, we noted that the sensitivity of the various glioma cells to protease inhibitors correlated with their sensitivity to the model ER stress inducer thapsigargin.[5] This observation prompted us to investigate the effects of nelfinavir and atazanavir on the expression of ER stress markers GRP78, CHOP, and caspase-4. Glioma cell lines were cultured in the presence of nelfinavir and atazanavir, and total cellular lysates were analyzed by Western blot with antibodies to GRP78, CHOP, and caspase-4. As shown in Fig. 1*C*, the treatment with nelfinavir and atazanavir strikingly increased GRP78 and CHOP protein levels in a concentration-dependent manner in all cell lines. Additionally, both drugs caused the activation of caspase-4, as indicated by the appearance of a cleaved caspase-4 protein with lower molecular weight.

To determine whether the ESR was involved in cell death induced by nelfinavir and atazanavir, we applied specific siRNAs to knock down the expression of either GRP78 or caspase-4. Glioma cells were transfected with siRNA and treated with the drug for 48 h, and the percentage of surviving cells was determined with the use of the colony formation assay. When GRP78 levels where reduced by siRNA, the cells became more sensitive, and there was less cell survival (Fig. 2*A*). In the case of caspase-4 siRNA, the opposite was observed: we found that the sensitivity of cells to drug treatment was significantly reduced (Fig. 2*A*). In addition, specific knockdown of the target was confirmed by Western blot analysis. As shown in Fig. 2*B*, siRNA to GRP78 reduced GRP78 protein levels; in the case of caspase-4, the specific siRNA not only reduced the overall amount of this target protein, but also prevented the appearance of the cleaved, i.e., activated, form of caspase-4.

Calcium homeostasis is an important function of the ER, and calcium disturbances result in ER stress. Thapsigargin, a widely used model inducer of ER stress, acts by inhibiting ER calcium ATPase activity, thereby causing an immediate spike in cytoplasmic calcium levels (25). To determine whether protease inhibitors would affect cytoplasmic calcium levels, we assessed the effect of acute exposure to nelfinavir and atazanavir. For this purpose, U251 cells were loaded with Fura-2/AM, exposed to 50 μmol/L nelfinavir or 100 μmol/L atazanavir, and the increase in cytoplasmic calcium levels was measured. As shown in Fig. 3, cells treated with nelfinavir and atazanavir did not display a rapid calcium spike, but rather maintained steady calcium levels after exposure to the drugs. In contrast, celecoxib, which is known to generate a rapid calcium spike (26, 27), was used as a positive control and caused an immediate cytoplasmic calcium spike (Fig. 3).

When tumor cells treated with nelfinavir or atazanavir were observed under light microscopy, we noticed striking morphologic changes (Fig. 4*A*). Following 24 h of treatment with either nelfinavir or atazanavir (only nelfinavir shown), large cytoplasmic vacuole-like structures could be observed. To investigate this phenomenon in greater detail, we applied transmission electron microscopy to nelfinavir-treated cells. Once again, large cytoplasmic vesicles were observed and were identified as grossly dilated, stressed ER. Similar effects on the ER were previously described by Dorner et al. (28) in Chinese hamster ovary cells, in which the synthesis of secreted proteins was excessively increased. In addition to the enlargement

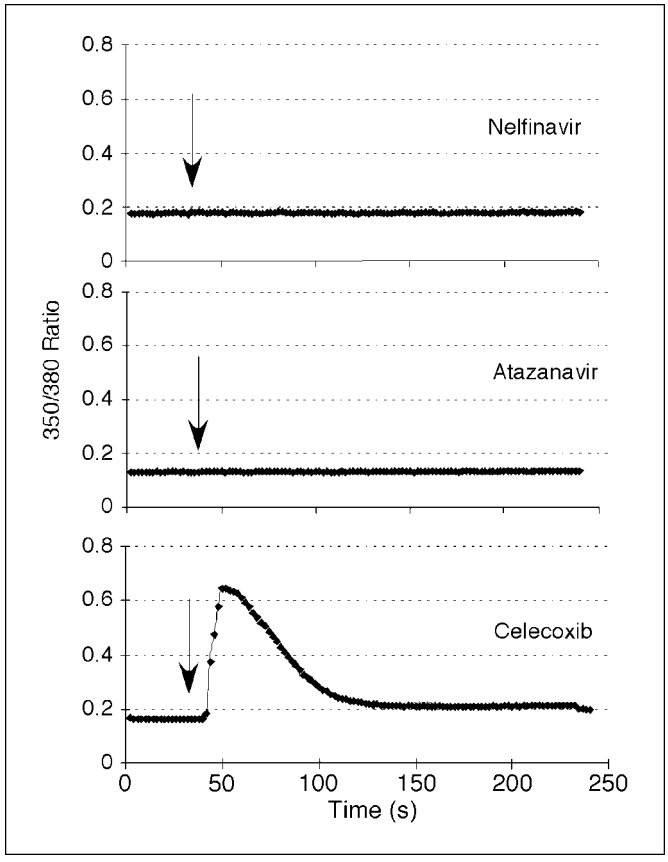

Figure 3. Nelfinavir and atazanavir do not affect cytoplasmic calcium levels during short-term treatment. U251 glioblastoma cells were treated with 30 μmol/L nelfinavir or 50 μmol/L atazanavir, and changes in cytoplasmic calcium levels were recorded. Short-term treatment (up to 4 min) with protease inhibitors revealed no increase in intracytoplasmic calcium levels. As a positive control, cells were exposed to 100 μmol/L of celecoxib, which is known to generate a rapid and prominent calcium spike (26). Shown are typical response curves from several repeats. *Arrows,* beginning of drug treatment.

[5] Unpublished data.

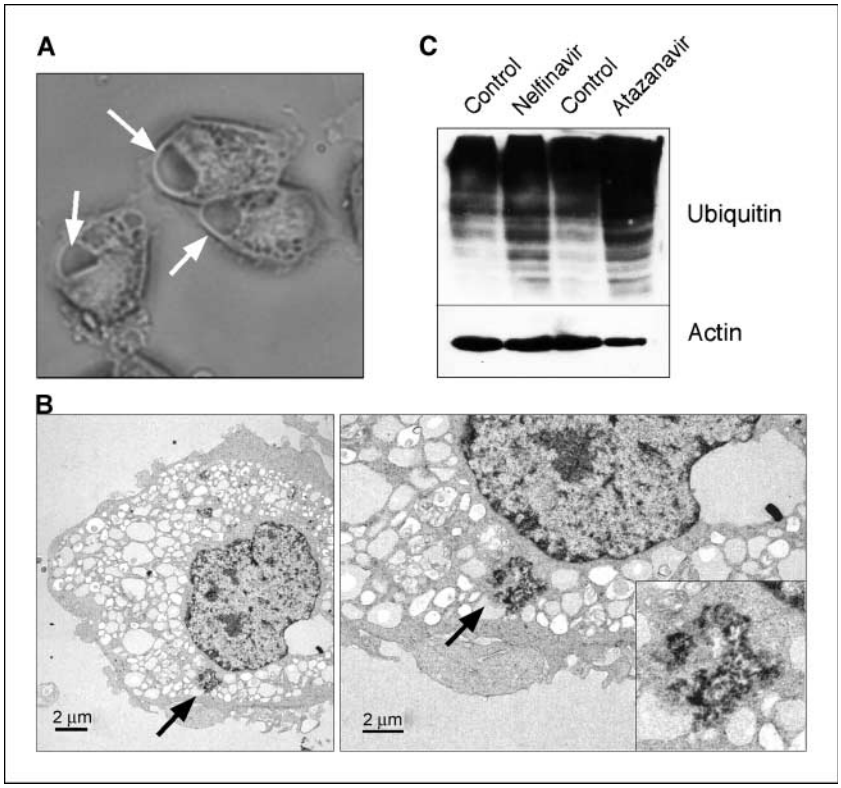

Figure 4. Nelfinavir and atazanavir cause inhibition of the proteasome. *A,* U251 glioblastoma cells were grown in the presence of 50 μmol/L nelfinavir for 24 h and visualized by light microscopy. *Arrows,* point to dilated ER cisternae. *B,* U251 cells in the presence of 50 μmol/L nelfinavir for 24 h were visualized by transition electron microscopy. *Left,* majority of the cell. *Right,* close-up on a part of the cell that contains an aggresome (*arrows* and *inset*). *C,* U251 cells were cultured in the presence or absence of 50 μmol/L nelfinavir and 80 μmol/L atazanavir for 24 h. Cellular lysates were prepared and subjected to Western blot analysis with antibodies to ubiquitin. Actin antibody was used as a loading control to verify equal amounts of lysate in each lane.

of the ER, we detected that a majority of drug-treated cells contained a structure consistent in appearance with an aggresome (Fig. 4*B*). Aggresomes are presumed to consist of an aggregation of ubiquitinated proteins due to the inhibition of proteasome activity (29, 30). Therefore, to investigate if the accumulation of polyubiquitinated proteins would occur during protease inhibitor treatment, lysates of cells treated with nelfinavir and atazanavir were subjected to Western blot analysis with antibody against ubiquitin. A prominent increase of polyubiquitinated proteins of various different sizes, represented by a smear on the blot, was observed in drug-treated cells (Fig. 4*C*), indicating that proteasome activity was indeed inhibited by these protease inhibitors.

A prominent feature of the ESR is a general, transient down-regulation of overall protein synthesis, in combination with selectively increased translation of ER stress proteins, such as GRP78 (31, 32). We therefore investigated whether nelfinavir would impair cellular translation by determining the incorporation of ^{35}S-methionine into newly translated proteins. As shown in Fig. 5*A*, 2 or 8 h of treatment with 30 μmol/L nelfinavir had very little effect on the rate of translation as compared with thapsigargin or the potent translational inhibitor cycloheximide, which both reduced ongoing translation by ~90% at 2 h. At 18 h, however, there was a noticeable decrease in protein translation rate in cells treated with nelfinavir; at 30 μmol/L, this reduction was 30% (Fig. 5*A*). Nelfinavir at 50 μmol/L and atazanavir at 80 μmol/L inhibited protein synthesis rate by >50% at 24 h (Fig. 5*B*). Interestingly, after 8, 18, and 24 h of treatment with nelfinavir and 24-h treatment with atazanavir, a prominent band with an apparent molecular weight of 78 kDa became visible. Via immunoprecipitation, we identified this band as GRP78 (Fig. 5*C*).

Thus far, our data indicated a model by which nelfinavir inhibited the proteasome, leading to the gradual accumulation of misfolded proteins, which caused ER stress and subsequent cell death. To further confirm this model, we employed the protein synthesis inhibitor cycloheximide, which would be expected to prevent the accumulation of newly synthesized, misfolded proteins, thereby averting the generation of ER stress. Toward this end, U251 glioma cells were treated with nelfinavir or atazanavir in the absence or presence of cycloheximide. After 24 h, light micrographs of all groups were taken. As shown in Fig. 5*D*, cell cultures treated with nelfinavir or atazanavir alone displayed striking morphologic changes in that the cells had lost most of their contact to the substratum, which led to cellular rounding and partial to complete detachment from the culture plate, consistent with the early phases of cellular death. In stark contrast, the presence of cycloheximide entirely prevented these drug-induced morphologic changes, and the cells maintained the same morphology as untreated control cells (Fig. 5*D*). We next investigated whether this obvious protective effect of cycloheximide could also be observed at the molecular level and, therefore, analyzed the amount of polyubiquitinated proteins and activation of caspase-4 by Western blot analysis. Consistent with the results above, cycloheximide prevented the accumulation of polyubiquitinated proteins, as well as the cleavage/activation of caspase-4, in nelfinavir- and atazanavir-treated cells (Fig. 5*D*).

Finally, in an effort to establish the antitumor effects of nelfinavir on malignant cells *in vivo* and to determine whether ER stress might be relevant in the *in vivo* setting as well, a xenograft nude mouse tumor model was used. U-87 malignant glioma cells were chosen because of their high *in vivo* tumorigenicity, and their genetic profile (p53 wild type, PTEN mutant) is consistent with a *de novo* glioblastoma (33–35). As shown in Fig. 6*A*, the daily treatment of tumor-bearing animals with nelfinavir significantly inhibited tumor growth during long-term (6 weeks) therapy. In

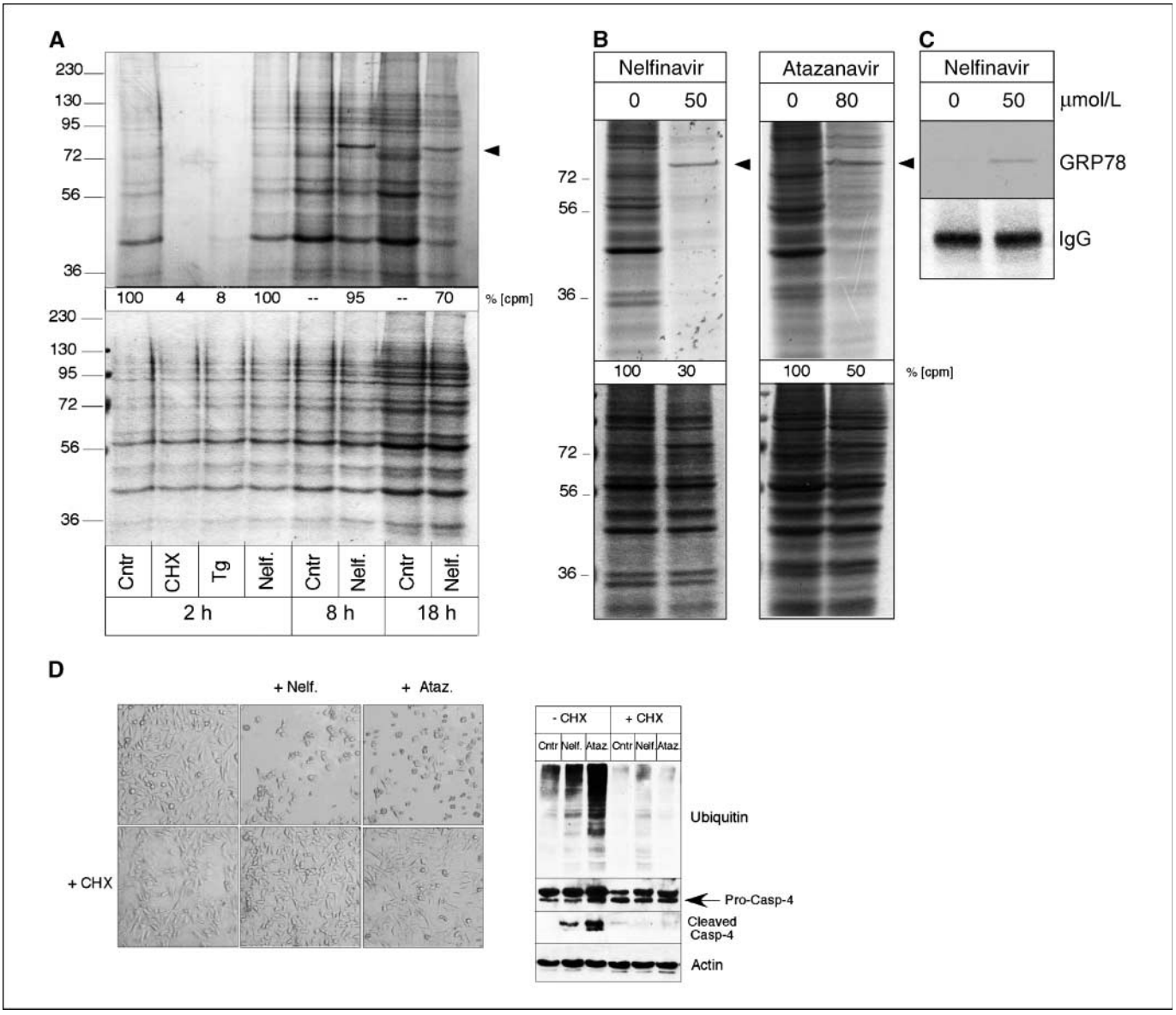

Figure 5. The role of protein synthesis in the action of PI. *A,* U251 cells were treated with 30 μmol/L of nelfinavir or 2.4 μmol/L thapsigargin (*Tg*) for the times indicated. As controls, cells remained untreated (*Cntr*) or were exposed to the potent protein synthesis inhibitor cycloheximide (*CHX*). During the final 30 min of each treatment condition, the culture medium was replaced with methionine-free growth medium supplemented with ^{35}S-methionine (20 μCi/mL) in the continued presence of the respective drug. Total cellular lysates were prepared, and equal amounts of each sample (30 μL) were separated by PAGE. *Top,* autoradiograph of the gel; *bottom,* the same gel stained with Coomassie blue. An aliquot from each sample was used to determine protein concentration, as well as the amount of incorporated ^{35}S-methionine; the resulting magnitude of incorporated radioactivity per milligram of total protein is shown as counts per minute (*cpm*), where the value from non–drug-treated cells at 2 h (*Cntr*) was set to 100%. *Arrowheads,* point to a prominently ^{35}S-labeled protein of 78 kDa. *B,* U251 cells were treated with 50 μmol/L of nelfinavir and 80 μmol/L atazanavir for 24 h, and ^{35}S-methionine incorporation was done as described in (*A*). *C,* the 78-kDa protein (*arrowheads* in *A* and *B*) was identified as GRP78 by immunoprecipitation analysis. *D,* U251 glioblastoma cells were exposed to 50 μmol/L nelfinavir and 80 μmol/L atazanavir for 24 h in the absence or presence of 50 μmol/L cycloheximide (*CHX*). Light micrographs of the cells show changes in morphology (*left*). Cellular lysates were prepared and subjected to Western blot analysis with antibodies to ubiquitin and caspase-4 (*casp-4*; basal levels of caspase-4 and its cleaved fragment were scanned at different exposures; *right*). Actin antibody was used as a loading control to verify equal amounts of lysate in each lane.

addition, after short-term treatment (96 h) of tumor-bearing animals with nelfinavir, highly elevated levels of the ER stress indicator protein CHOP could be detected in the tumor tissue from these animals; whereas non–drug-treated animals displayed only barely detectable amounts of this protein (Fig. 6*B*). In addition, the highly elevated amount of CHOP protein after nelfinavir treatment correlated with significantly increased apoptosis in the tumor tissue, whereas tumors from vehicle-treated animals did not display elevated levels of apoptosis (Fig. 6*B*).

Discussion

Despite growing interest in HIV-1 protease inhibitors (PI) as anti-cancer drugs, the anticancer mechanism of action of this group of chemical compounds is unknown. In our current study, we show that the PIs nelfinavir and atazanavir induce glioma cell death by triggering the ESR. In general, the main purpose of the ESR is to alleviate specific disturbances, for instance, changes in the ionic conditions of the ER or accumulation of misfolded proteins, and restore proper homeostasis. Major components of this

protective function are chaperone proteins, such as GRP78 (17). However, if the insult is too severe and cannot be eliminated, the ESR will initiate cell death via its proapoptotic components, which include CHOP and caspase-4 (18, 19).

Recently, Gills et al. (36) have evaluated seven Food and Drug Administration–approved HIV PIs (amprenavir, atazanavir, indinavir, lopinavir, nelfinavir, ritonavir, and saquinavir) against lung cancer and found that nelfinavir was the most potent. Therefore, we used nelfinavir as one of the first-generation and atazanavir as one of the newer generation PIs, and we found that both of these drugs potently triggered ESR. At the molecular level, this effect was revealed by the robust induction of the ESR markers GRP78 and CHOP and the activation of ESR-associated caspase-4 (Fig. 1). In addition, both drugs caused dilated ER compartments (Fig. 4), which is a typical morphologic feature of cells experiencing severe ER stress (28).

Our siRNA experiments provided evidence that the induction of ESR indeed plays a critical role in the anticancer activity of these PIs. Specifically, knockdown of GRP78 (the protective component of the ESR) enhanced cell death by nelfinavir and atazanavir, whereas knockdown of caspase-4 (a proapoptotic component of the ESR) significantly increased cell survival after treatment with these drugs (Fig. 2). Both outcomes are consistent with the prosurvival role of GRP78 and the proapoptotic role of caspase-4 in the ESR and reveal a direct involvement of this process in PI action. Similar siRNA-type approaches by other investigators have shown a prominent role of the ESR in cell death induced by other categories of drugs as well. For example, knockdown of GRP78 resulted in decreased survival of gastric adenocarcinoma cells after treatment with celecoxib, a cyclooxygenase-2 inhibitor (37), and sensitized breast cancer cells to etoposide-mediated cell death (38). Conversely, knockdown of caspase-4 was shown to protect pancreatic cancer cells from apoptosis induced by bortezomib, a proteasome inhibitor that is clinically used in the therapy of multiple myeloma (29).

Our investigation of protein translation rates showed a moderate inhibition of overall protein synthesis after prolonged incubation of cells with PIs, concomitant with selectively increased expression of GRP78 (Fig. 5). Such differential effects are typical indicators of the ESR, although the severity and timing of inhibition may vary greatly depending on the insult. For example, shutdown of general translation by thapsigargin, a potent inhibitor of ER calcium pumps, is rapid and very efficient due to the immediate increase in cytosolic calcium concentrations (ref. 39; see also Fig. 5). On the

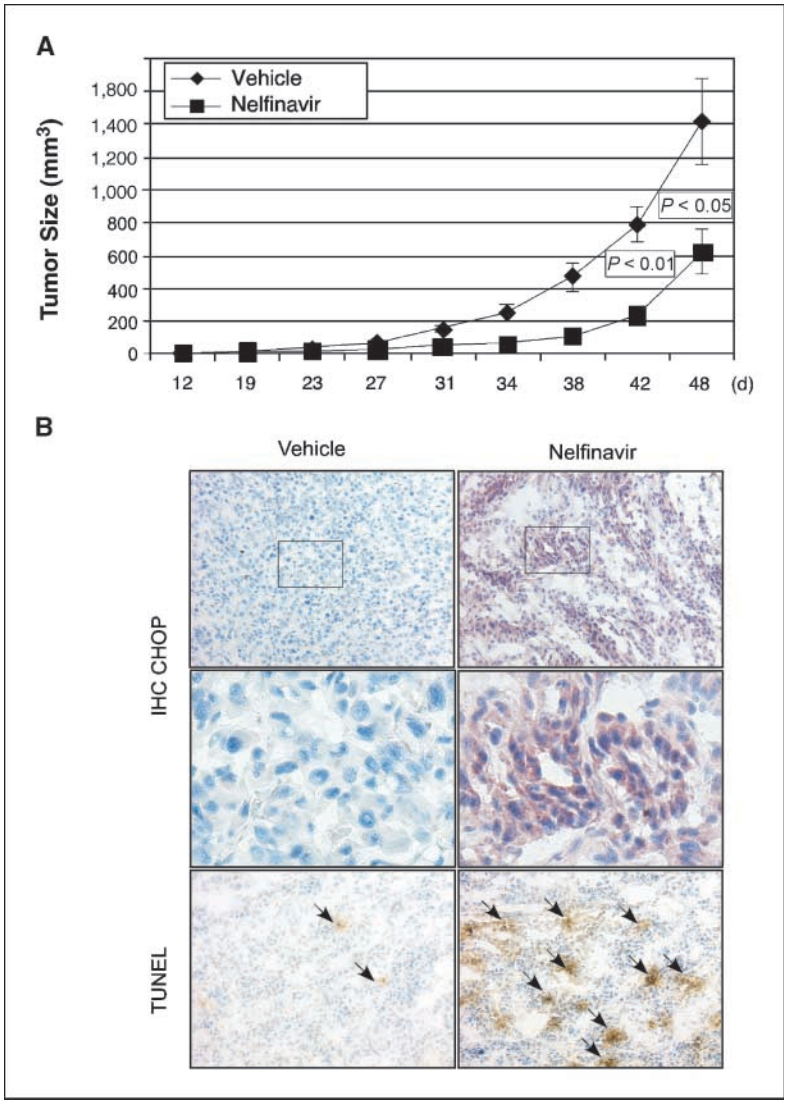

Figure 6. Nelfinavir inhibits tumor growth and stimulates ESR and apoptosis in tumor cells *in vivo. A,* nude mice were implanted s.c. with U87 glioblastoma cells. Once palpable tumors had formed, the animals received daily gavage with nelfinavir or the same volume of solvent (25% ethanol; 40 mg/kg). Tumor size was determined every 3 to 6 d. *Points,* mean tumor volume in each group; *bars,* SE; $n = 5$. *P* values between control and nelfinavir-treated animals on day 42 and 48 are indicated. *B,* Nude mice were implanted s.c. with U87 glioblastoma cells. Once tumors had reached a volume of 500 mm^3, two animals each received either nelfinavir or vehicle alone (25% ethanol) for 96 h (120 mg/kg). Thereafter, all four animals were sacrificed, and their tumors were analyzed by immunohistochemical staining for CHOP protein as well as TUNEL assay for cell death/apoptosis. *Top,* expression of CHOP protein. *Small black rectangles,* enlarged areas of the same photograph shown below in the middle. *Bottom,* cell death (*arrows*, examples of TUNEL-positive, i.e., apoptotic, cells). In all cases, representative sections are shown.

other hand, bortezomib, which triggers ESR via the inhibition of the proteasome, leads to a gradual buildup of misfolded protein levels and, therefore, requires longer incubation times and affects general translation rates only moderately (29). In comparison, we find that the kinetics of translational inhibition by nelfinavir resemble those of bortezomib and do not involve rapid changes in cytoplasmic calcium (Fig. 3). This similarity is noteworthy in light of our observation that treatment of glioblastoma cells with nelfinavir and atazanavir results in the accumulation of polyubiquitinated proteins and aggresome formation (Fig. 4), which are typical indicators of proteasome inhibition. Furthermore, reports by others have shown that nelfinavir impairs proteasome function in human hepatoma cells (40), and two further PIs, saquinavir and ritonavir, were shown to inhibit proteasomal activity in prostate carcinoma and thymoma cell lines (6, 10). Thus, our results provide additional support for the emerging view that some, if not all, HIV-1 PIs act as inhibitors of the proteasome. Furthermore, they suggest that this function might participate in triggering ESR, in agreement with several reports linking the inhibition of proteasomal activity by bortezomib and other established proteasome inhibitors to the accumulation of misfolded proteins and subsequent ESR (29, 41, 42).

The above results are consistent with the following proposed model of PI antitumor action: PIs inhibit the proteasome, which prevents the degradation of proteins; at the same time, general protein synthesis continues to proceed, which results in the accumulation of unfolded/misfolded proteins. This, in turn, triggers ESR as the cell's attempt to neutralize impending proteotoxicity. As part of this protective response, the ER chaperone GRP78 is induced, and the rate of new protein synthesis is slowed. However, because proteins cannot be degraded due to constant inhibition of the proteasome in the continued presence of the drug, the protective arm of the ESR eventually is overwhelmed, and the balance is shifted toward its proapoptotic components (CHOP and caspase-4), which initiate cell death. This order of events is also supported by our finding that cycloheximide efficiently blocks the induction of ESR by PIs, i.e., PI-induced morphologic changes, accumulation of polyubiquitinated proteins, and cleavage of caspase-4 do not take place in the presence of this nondiscriminatory inhibitor of total protein synthesis (Fig. 5), quite likely due to the cell's inability to accumulate newly synthesized unfolded/misfolded proteins under these conditions.

An important question resulting from our results was whether the effects observed *in vitro* would also take place *in vivo*. Two of our results indicate that the answer is yes. First, in our xenograft tumor model, nelfinavir significantly inhibited U87 glioma growth *in vivo*. Second, nelfinavir also caused robust induction of the ESR indicator CHOP and apoptosis in tumors from these animals (Fig. 6). Taken together, these results reveal that the antitumor and ESR-inducing effects of nelfinavir are not restricted to *in vitro* conditions, but also take place in the *in vivo* setting. Additionally, our *in vitro* results show that the induction of ESR markers, as well as the noticeable inhibition of glioblastoma cell proliferation, by nelfinavir can take place at concentrations of 6 μmol/L and below (Fig. 1*A* and *B*). Such concentrations are known to be attainable clinically (43, 44) and, therefore, open the prospect that antitumor effects of nelfinavir might be achievable in cancer patients as well. Cancer cells generally display elevated metabolic rates and increased rates of protein synthesis. Because of this distinction, the consequences of proteasome inhibition would be expected to be more deleterious in cancer cells than in normal cells. A few recent studies indeed seem to support this concept. For example, it was shown that the proteasome inhibitor bortezomib induced aggresome formation and apoptosis in pancreatic carcinoma cells, but did not exert these effects in normal pancreatic epithelial cells *in vitro* or *in vivo* (30). Similarly, the PI ritonavir potently stimulated apoptosis in various tumor cell lines, whereas nontransformed cell lines and terminally differentiated bone marrow macrophages were comparatively resistant to this effect (6).

The use of PIs in gliomas has a number of potential advantages and disadvantages. PIs are small molecules that should cross the blood-brain barrier (BBB) readily. They have already been shown (albeit, indirectly) to have activity in the central nervous system (CNS), as the number of HIV patients with CNS lymphomas has decreased significantly since the initiation of HAART (2). Laurent et al. have shown that ritonavir penetrated across the BBB and achieved adequate concentrations in the CNS in an intracranial glioma model (7). Yilmaz et al. (45) have measured cerebrospinal fluid (CSF) levels of both nelfinavir and saquinavir, with better CSF concentrations of nelfinavir, compared with saquinavir.

One major potential risk for PIs is the development of insulin resistance with progression to type II diabetes (46, 47). In this regard, it is interesting to note that several recent papers have established ER stress as a key link between obesity, insulin resistance, and type II diabetes (48, 49). In particular, it was shown that obese mice experienced chronic ESR, which lead to insulin resistance and type 2 diabetes, and these pathologic metabolic consequences could be prevented by an orally active chemical chaperone that alleviated ER stress in cells and whole animals (48, 49) The development of insulin resistance may be problematic in brain tumor patients who are often on systemic steroids. Many of these patients may have their systemic blood sugar level increased with the combination of Decadron and PIs; how significant this elevation becomes will need to be determined.

Acknowledgments

Received 2/27/2007; revised 9/7/2007; accepted 9/14/2007.

Grant support: Accelerate Brain Cancer Cure (to T.C. Chen and A.H. Schönthal) and from the Margaret E. Early Medical Research Trust (to A.H. Schönthal).

The costs of publication of this article were defrayed in part by the payment of page charges. This article must therefore be hereby marked *advertisement* in accordance with 18 U.S.C. Section 1734 solely to indicate this fact.

We are grateful to Frank B. Furnari and Webster K. Cavenee (Ludwig Institute for Cancer Research, La Jolla, CA) for the glioblastoma cell lines. We thank Dr. Amy Lee for the initial aliquots of caspase-4 antibody and siGRP78, as well as discussions about ESR. We also thank the University of Southern California Glioma Research Group, in particular Dr. Florence Hofman, for discussions and comments during the work on this project.

References

1. Perrin L, Telenti A. HIV treatment failure: testing for HIV resistance in clinical practice. Science 1998;280:1871–3.
2. Sgadari C, Barillari G, Toschi E, et al. HIV protease inhibitors are potent anti-angiogenic molecules and promote regression of Kaposi sarcoma. Nat Med 2002;8:225–32.
3. Esposito V, Palescandolo E, Spugnini EP, et al. Evaluation of antitumoral properties of the protease inhibitor indinavir in a murine model of hepatocarcinoma. Clin Cancer Res 2006;12:2634–9.
4. Yang Y, Ikezoe T, Takeuchi T, et al. HIV-1 protease inhibitor induces growth arrest and apoptosis of human prostate cancer LNCaP cells *in vitro* and *in vivo* in conjunction with blockade of androgen receptor STAT3 and AKT signaling. Cancer Sci 2005;96:425–33.
5. Ikezoe T, Saito T, Bandobashi K, Yang Y, Koeffler HP, Taguchi H. HIV-1 protease inhibitor induces growth arrest and apoptosis of human multiple myeloma cells

via inactivation of signal transducer and activator of transcription 3 and extracellular signal-regulated kinase 1/2. Mol Cancer Ther 2004;3:473–9.
6. Gaedicke S, Firat-Geier E, Constantiniu O, et al. Antitumor effect of the human immunodeficiency virus protease inhibitor ritonavir: induction of tumor-cell apoptosis associated with perturbation of proteasomal proteolysis. Cancer Res 2002;62:6901–8.
7. Laurent N, de Bouard S, Guillamo JS, et al. Effects of the proteasome inhibitor ritonavir on glioma growth *in vitro* and *in vivo*. Mol Cancer Ther 2004;3:129–36.
8. Ikezoe T, Daar ES, Hisatake J, Taguchi H, Koeffler HP. HIV-1 protease inhibitors decrease proliferation and induce differentiation of human myelocytic leukemia cells. Blood 2000;96:3553–9.
9. Ikezoe T, Hisatake Y, Takeuchi T, et al. HIV-1 protease inhibitor, ritonavir: a potent inhibitor of CYP3A4, enhanced the anticancer effects of docetaxel in androgen-independent prostate cancer cells *in vitro* and *in vivo*. Cancer Res 2004;64:7426–31.
10. Pajonk F, Himmelsbach J, Riess K, Sommer A, McBride WH. The human immunodeficiency virus (HIV)-1 protease inhibitor saquinavir inhibits proteasome function and causes apoptosis and radiosensitization in non–HIV-associated human cancer cells. Cancer Res 2002;62:5230–5.
11. Pore N, Gupta AK, Cerniglia GJ, Maity A. HIV protease inhibitors decrease VEGF/HIF-1α expression and angiogenesis in glioblastoma cells. Neoplasia 2006;8:889–95.
12. Jiang W, Mikochik PJ, Ra JH, et al. HIV protease inhibitor nelfinavir inhibits growth of human melanoma cells by induction of cell cycle arrest. Cancer Res 2007; 67:1221–7.
13. Gupta AK, Cerniglia GJ, Mick R, McKenna WG, Muschel RJ. HIV protease inhibitors block Akt signaling and radiosensitize tumor cells both *in vitro* and *in vivo*. Cancer Res 2005;65:8256–65.
14. Pati S, Pelser CB, Dufraine J, Bryant JL, Reitz MS, Jr., Weichold FF. Antitumorigenic effects of HIV protease inhibitor ritonavir: inhibition of Kaposi sarcoma. Blood 2002;99:3771–9.
15. Boyce M, Yuan J. Cellular response to endoplasmic reticulum stress: a matter of life or death. Cell Death Differ 2006;13:363–73.
16. Wu J, Kaufman RJ. From acute ER stress to physiological roles of the unfolded protein response. Cell Death Differ 2006;13:374–84.
17. Li J, Lee AS. Stress induction of GRP78/BiP and its role in cancer. Curr Mol Med 2006;6:45–54.
18. Hitomi J, Katayama T, Eguchi Y, et al. Involvement of caspase-4 in endoplasmic reticulum stress-induced apoptosis and Abeta-induced cell death. J Cell Biol 2004;165:347–56.
19. Oyadomari S, Mori M. Roles of CHOP/GADD153 in endoplasmic reticulum stress. Cell Death Differ 2004;11: 381–9.
20. Harlow E, Lane D. Using antibodies: a laboratory manual. Cold Spring Harbor (NY): Cold Spring Harbor Laboratory Press; 1999. p. 267–309.
21. Abramoff MD, Magalhaes PJ, Ram SJ. Image processing with ImageJ. Biophotonics Int 2004;11:36–42.
22. Heatwole VM. TUNEL assay for apoptotic cells. Methods Mol Biol 1999;115:141–8.
23. Grynkiewicz G, Poenie M, Tsien RY. A new generation of Ca^{2+} indicators with greatly improved fluorescence properties. J Biol Chem 1985;260:3440–50.
24. Pyrko P, Soriano N, Kardosh A, et al. Downregulation of survivin expression and concomitant induction of apoptosis by celecoxib and its non-cyclooxygenase-2-inhibitory analog, dimethyl-celecoxib (DMC), in tumor cells *in vitro* and *in vivo*. Mol Cancer 2006;5:19.
25. Gallego-Sandin S, Novalbos J, Rosado A, et al. Albumin prevents mitochondrial depolarization and apoptosis elicited by endoplasmic reticulum calcium depletion of neuroblastoma cells. Eur J Pharmacol 2005; 520:1–11.
26. Johnson AJ, Hsu AL, Lin HP, Song X, Chen CS. The cyclo-oxygenase-2 inhibitor celecoxib perturbs intracellular calcium by inhibiting endoplasmic reticulum Ca^{2+}-ATPases: a plausible link with its anti-tumour effect and cardiovascular risks. Biochem J 2002;366:831–7.
27. Pyrko P, Kardosh A, Liu Y-T, et al. Calcium-activated ER stress as a major component of tumor cell death induced by 2,5-dimethyl-celecoxib (DMC), a non-coxib analog of celecoxib. Mol Cancer Ther 2007;6:1262–75.
28. Dorner AJ, Wasley LC, Kaufman RJ. Increased synthesis of secreted proteins induces expression of glucose-regulated proteins in butyrate-treated Chinese hamster ovary cells. J Biol Chem 1989;264:20602–7.
29. Nawrocki ST, Carew JS, Dunner K, Jr., et al. Bortezomib inhibits PKR-like endoplasmic reticulum (ER) kinase and induces apoptosis via ER stress in human pancreatic cancer cells. Cancer Res 2005;65: 11510–9.
30. Nawrocki ST, Carew JS, Pino MS, et al. Aggresome disruption: a novel strategy to enhance bortezomib-induced apoptosis in pancreatic cancer cells. Cancer Res 2006;66:3773–81.
31. Luo S, Baumeister P, Yang S, Abcouwer SF, Lee AS. Induction of Grp78/BiP by translational block: activation of the Grp78 promoter by ATF4 through and upstream ATF/CRE site independent of the endoplasmic reticulum stress elements. J Biol Chem 2003;278: 37375–85.
32. Ma Y, Hendershot LM. The role of the unfolded protein response in tumour development: friend or foe? Nat Rev Cancer 2004;4:966–77.
33. Van Meir EG, Kikuchi T, Tada M, et al. Analysis of the p53 gene and its expression in human glioblastoma cells. Cancer Res 1994;54:649–52.
34. Furnari FB, Lin H, Huang HS, Cavenee WK. Growth suppression of glioma cells by PTEN requires a functional phosphatase catalytic domain. Proc Natl Acad Sci U S A 1997;94:12479–84.
35. Chen TC, Apuzzo MLJ. Malignant progression in gliomas. Park Ridge: American Association of Neurological Surgeons; 1995. p. 181–9.
36. Gills J, Lopiccolo J, Abu-Asab MS, Shoemaker R, Borojerdi J, Dennis PA. HIV protease inhibitors as cancer therapeutics: is off-the-shelf right on target? AACR Meeting Abstracts 2006.
37. Tsutsumi S, Namba T, Tanaka KI, et al. Celecoxib upregulates endoplasmic reticulum chaperones that inhibit celecoxib-induced apoptosis in human gastric cells. Oncogene 2006;25:1018–29.
38. Dong D, Ko B, Baumeister P, et al. Vascular targeting and antiangiogenesis agents induce drug resistance effector GRP78 within the tumor microenvironment. Cancer Res 2005;65:5785–91.
39. Wong WL, Brostrom MA, Kuznetsov G, Gmitter-Yellen D, Brostrom CO. Inhibition of protein synthesis and early protein processing by thapsigargin in cultured cells. Biochem J 1993;289:71–9.
40. Hamel FG, Fawcett J, Tsui BT, Bennett RG, Duckworth WC. Effect of nelfinavir on insulin metabolism, proteasome activity and protein degradation in HepG2 cells. Diabetes Obesity and Metabolism 2006;8:661–8.
41. Lee AH, Iwakoshi NN, Anderson KC, Glimcher LH. Proteasome inhibitors disrupt the unfolded protein response in myeloma cells. Proc Natl Acad Sci U S A 2003;100:9946–51.
42. Fribley A, Wang CY. Proteasome inhibitor induces apoptosis through induction of endoplasmic reticulum stress. Cancer Biol Ther 2006;5:745–8.
43. Smith PF, Robbins GK, Shafer RW, et al. Pharmacokinetics of nelfinavir and efavirenz in antiretroviral-naive, human immunodeficiency virus-infected subjects when administered alone or in combination with nucleoside analog reverse transcriptase inhibitors. Antimicrob Agents Chemother 2005;49:3558–61.
44. Regazzi M, Maserati R, Villani P, et al. Clinical pharmacokinetics of nelfinavir and its metabolite M8 in human immunodeficiency virus (HIV)-positive and HIV-hepatitis C virus–coinfected subjects. Antimicrob Agents Chemother 2005;49:643–9.
45. Yilmaz A, Fuchs D, Hagberg L, et al. Cerebrospinal fluid HIV-1 RNA, intrathecal immunoactivation, and drug concentrations after treatment with a combination of saquinavir, nelfinavir, and two nucleoside analogues: the M61022 study. BMC Infect Dis 2006;6:63.
46. Nolan D. Metabolic complications associated with HIV protease inhibitor therapy. Drugs 2003;63:2555–74.
47. Rudich A, Ben-Romano R, Etzion S, Bashan N. Cellular mechanisms of insulin resistance, lipodystrophy and atherosclerosis induced by HIV protease inhibitors. Acta Physiol Scand 2005;183:75–88.
48. Ozcan U, Cao Q, Yilmaz E, et al. Endoplasmic reticulum stress links obesity, insulin action, and type 2 diabetes. Science 2004;306:457–61.
49. Ozcan U, Yilmaz E, Ozcan L, et al. Chemical chaperones reduce ER stress and restore glucose homeostasis in a mouse model of type 2 diabetes. Science 2006;313:1137–40.
50. Kardosh A, Soriano N, Liu YT, et al. Multitarget inhibition of drug-resistant multiple myeloma cell lines by dimethyl-celecoxib (DMC), a non–COX-2 inhibitory analog of celecoxib. Blood 2005;106:4330–8.